Structural Engineering and Mechanics, Vol. 5, No. 5 (1997) 625-634
DOI: http://dx.doi.org/10.12989/sem.1997.5.5.625

Finite element analysis of RC beam-column joints with high-strength materials

H. Noguchi† and T. Kashiwazaki‡

Department of Architecture, Chiba University, 1-33 Yayoi-cho, Inage-ku, Chiba-City 263, Japan

Abstract. Reinforced concrete (RC) interior beam-column joints with high-strength materials: concrete compressive strength of 100 MPa and the yield strength of longitudinal bars of 685 MPa, were analyzed using three-dimensional (3-D) nonlinear finite element method (FEM). Specimen OKJ3 of joint shear failure type was a plane interior joint, and Specimen I2 of beam flexural failure type was a 3-D interior joint with transverse beams. Though the analytical initial stiffness was higher than experimental one, the analytical results gave a good agreement with the test results on the maximum story shear forces, the failure mode.

Key words: reinforced concrete; beam-column joints; high-strength materials; shear strength; three-dimensional analysis; finite element method.

1. Introduction

Beam-column joints in a RC building are generally subjected to two-directional forces during an earthquake. The shear strength of the joints under two-directional seismic forces have not been known clearly and rationally in the previous studies. The shear resistance mechanisms of such a joint become 3-D problems, and the joint is confined by joint lateral reinforcement, transverse beams, a slab and a column axial force. It is necessary to grasp the shear behavior of the joint subjected to two-directional seismic forces from not only experimental studies but also analytical studies.

Design Guidelines for Earthquake Resistant RC Buildings Based on Ultimate Strength Concept were published by Architectural Institute of Japan (AIJ 1990) (AIJ Guidelines) suggested that such a 3-D interior beam-column joint should be designed for two principal directions independently. The shear design provisions of the joint in AIJ Guidelines are based on the previous experimental results using normal strength materials. Therefore, it is necessary to establish the more rational shear design method for the joints under two-directional seismic forces from the analytical understanding of the joint shear resistance mechanisms including high-strength materials.

† Professor
‡ Research Associate

2. Outline of FEM analysis

2.1. Reference specimen for 3-D FEM analysis

Previous interior beam-column joint test specimens OKJ3 (tested by Kashiwazaki, *et al.* 1991) and I2 (tested by Lee, *et al.* 1992) using high-strength materials were selected as the references for this study. As for specimen OKJ3 of the plane joint without transverse beams, joint shear failure occurred before beam flexural yielding in the test. But as for specimen I2 of the 3-D joint with transverse beams, beam flexural failure occurred before joint shear failure.

The details of one-third scaled specimens OKJ3 and I2 are shown in Table 1 and 2. The

Table 1 Properties of specimens

Specimen		Two-dimensional OKJ3	Three-dimensional I2
Beam	Top bars	10-D13	8-D16
	Bottom bars	10-D13	8-D16
	Stirrups	2-D6 @50, pw=0.63(%)	2-U6.4 @35, pw=0.86(%)
Column	Top bars	22-D13	16-D19
	hoops	2-D6 @40, pw=0.53(%)	2-U6.4 @40, pw=0.50(%)
Joint	Hoops	4-D6×3 sets @50 pw=0.54(%)	4-ϕ6×2 sets @30 pw=0.39(%)

Table 2 Material properties

a) Concrete (unit in MPa and μ)

Specimen	Two-dimensional OKJ3	Three-dimensional I2
Scent modulus	43300	39200
Compressive strength	107	99
Strain at compressive strength	2860	2752
Spliting strength	6.0	4.2

b) Reinforcement (unit in MPa and μ)

Specimen	Two-dimensional OKJ3		Three-dimensional I2			
Reinforcement	D6	D13	D16	D19	U6.4	ϕ6
Young's Modulus, $\times 10^5$	1.82	1.86	1.82	1.81	1.86	1.86
Yield strength	955	717	798	746	1307	356
Maximum strength	1140	766	859	806	1397	431

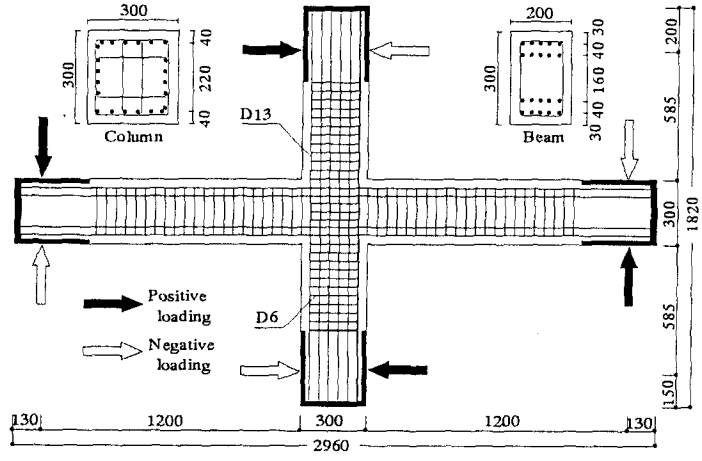

Fig. 1 Arrangement of reinforcement, OKJ3.

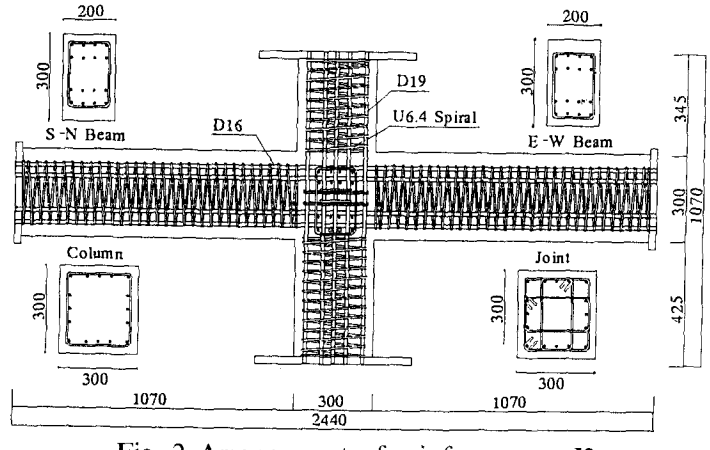

Fig. 2 Arrangement of reinforcement, I2.

concrete compressive strength was 107 and 99 MPa for specimens OKJ3 and I2, respectively. The yield strength of beam main bars was 717 (D13) and 798 MPa (D16) for specimens OKJ3 and I2, respectively. The yield strength of joint lateral bars was 955 MPa for D6 in specimen OKJ3 and 1307 MPa for U6.4 in specimen I2, respectively. The reinforcement arrangement of specimens OKJ3 and I2 are shown in Figs. 1 and 2. The joint lateral reinforcement ratio was 0.54% and 0.39% for specimens OKJ3 and I2, respectively. Reversed cyclic loads were applied to two beam-ends of specimen OKJ3, and a constant axial load of 85 tf was applied to the column (axial stress $\sigma_0 = 0.1\sigma_B$, σ_B: concrete compressive strength). Three-dimensional reversed cyclic loads were applied to the top of the column until the story drift angle of 1/25 rad.. A constant axial load of 32.5 tf was applied to the top of the column.

2.2. *Analytical method and material models*

This analysis was carried out by using a 3-D nonlinear FEM program (Uchida, *et al.* 1992, Yonezawa, *et al.* 1994). Figs. 3 and 4 show the modeling of specimens OKJ3 and I2, respectively.

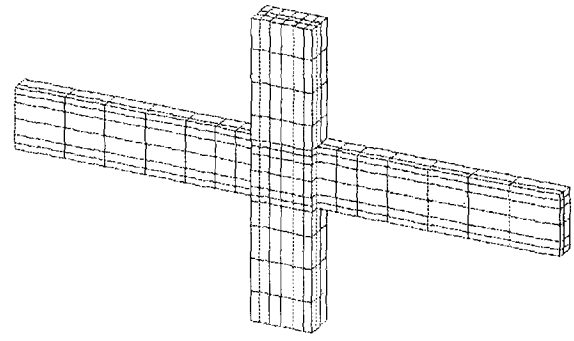

Fig. 3 Finite element idealization, OKJ3.

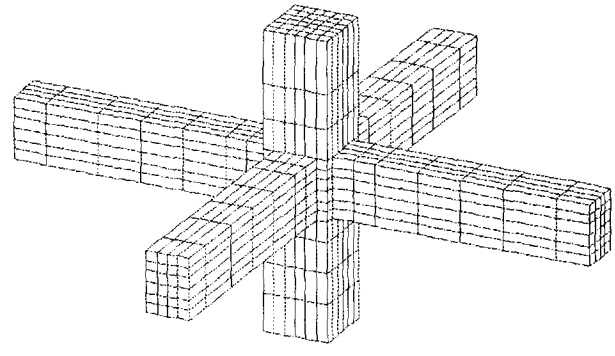

Fig. 4 Finite element idealization, I2.

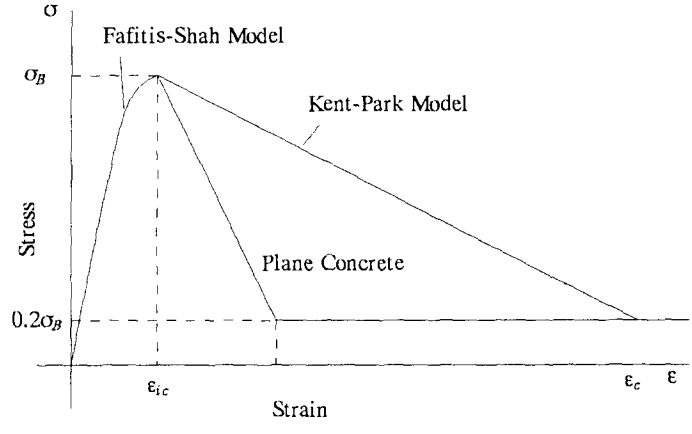

Fig. 5 Compressive stress-strain relationships of concrete.

The half areas of specimens OKJ3 and I2 under one-directional loading were analyzed using the symmetrical condition. The boundary conditions for the top and bottom of the column and beam ends were set up according to the experiment. The following nonlinear constitutive models for high-strength materials were introduced into the 3-D FEM program.

2.2.1. Concrete

Concrete was represented by 8-node solid elements. Concrete was assumed as orthotropic hypoelastic model based on the equivalent uniaxial strain concept modified by Murray, *et al.* for the 3-D FEM analysis. The failure was judged by the five parameter criterion which was added two parameters to the three parameter criterion proposed by Willam and Warnke. The five parameters were decided using the panel experiment by Kupfer. Fafitis-Shah model (Fafitis, *et al.* 1985) was used for the ascending compressive stress-strain relationships of high-strength concrete, as shown in Fig. 5. Confined effect by lateral reinforcement on the compressive descending stress-strain relationships were represented by Kent-Park model (Kent, *et al.* 1971). Poisson's ratio of concrete was modeled as a function of compressive strain proposed by Murray. Cracks in concrete elements were represented by the smeared crack model. After cracking, tension cut-off was assumed, and the stiffness normal to a crack direction was set to be zero. The reduction factor of concrete compressive strength of cracked concrete high-strength proposed by Ihzuka and Noguchi (Ihzuka, *et al.* 1992) was used.

2.2.2. Reinforcement and bond

The longitudinal and lateral reinforcement in columns and beams was assumed to be a linear element. The stress-strain relationships of the longitudinal and lateral reinforcement were assumed to be bilinear and trilinear, respectively. The bond between the longitudinal reinforcement and concrete was assumed as perfect bond. The slippage of beam longitudinal reinforcement through a joint was not considered.

Test results were used for the properties of concrete and reinforcing bars in the analysis.

3. Analytical results

3.1. Restoring force characteristics

The analytical story shear force-story displacement relationships of the plane interior beam-column joint specimen OKJ3 and the 3-D joint specimen I2 are shown as compared with the test results in Figs. 6 and 7, respectively. The *P-δ* effect caused by loading to the top of the

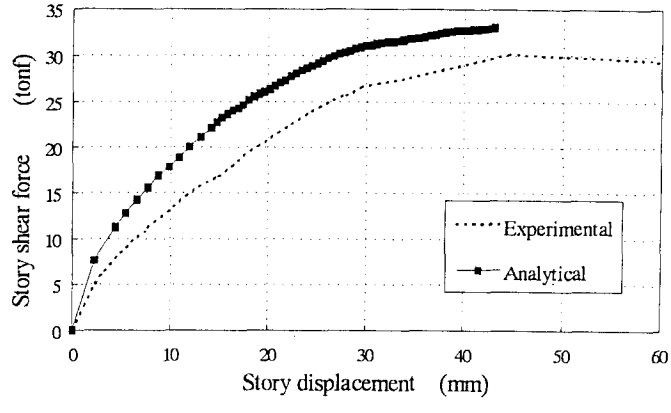

Fig. 6 Story shear force-story displacement relationships, OKJ3.

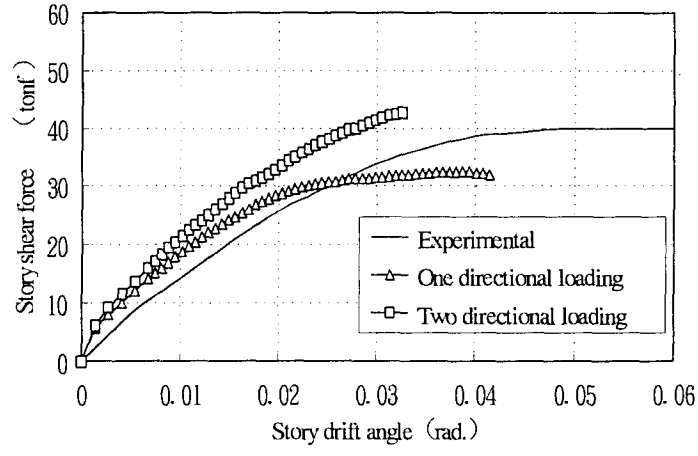

Fig. 7 Story shear force-story displacement relationships, I2.

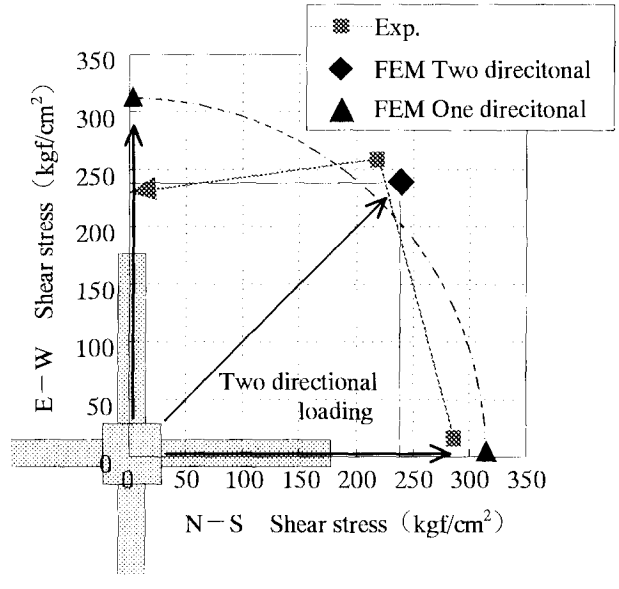

Fig. 8 Loci of shear stress in the joint, I2.

column was considered in the analysis and experiment. The test results show the envelope curves of hysteresis loops in the *N-S* direction. In the analysis of specimen I2, both one-directional and two-directional loading were subjected to the specimen.

The analytical initial stiffness was higher than the experimental one. It is considered that the local flexural crack on the critical section of the beam was not represented using the smeared rack model. The analytical maximum story shear force (Ps=33.5tf) of specimen OKJ3 were higher than the test results (Ps=29.9tf) about 10 percent. The yielding of beam longitudinal reinforcement was not observed in the analysis, and the stress condition of a few joint concrete elements reached strain softening after the peak stress at the maximum story shear force. It was recognized that the joint shear failure occurred in specimen OKJ3 similarly to the experiment. The analytical maximum story shear force (Ps=42.7tf) of specimen I2 under one-directional loading were higher

than the test results (Ps=40.0tf) about 7%. Under two-directional loading, the analytical maximum story shear force component in the *N-S* direction showed a lower value (Ps=32.6 tf).

The loci of the joint input shear stresses are shown in Fig. 8. Under two-directional loading, the analytical joint input shear stress component (τ_u=236 kgf/cm^2) in the *N-S* direction was lower than the test result (τ_u=284 kgf/cm^2) and the analytical result (τ_u=313 kgf/cm^2) under one-directional loading. But the analytical maximum shear stress under two-directional (45 degree) loading (τ_u=334 kgf/cm^2) was higher than that (=313 kgf/cm^2) under one-directional loading. In the test, the reduction of the maximum shear stress component in the *N-S* direction was observed in the process under the *W-E* direction loading keeping the displacement caused by the *N-S* direction loading. From the comparison in the two-directional (45 degree) loading, the analytical maximum shear stress gave a reasonable agreement with the test result. The analytical failure mode was beam flexural yielding nearly at the story drift angle of 1/33 rad., and it was corresponding to the test result.

3.2. Strain in reinforcement

Strain distributions of beam longitudinal reinforcement (the first layer of top bars) through

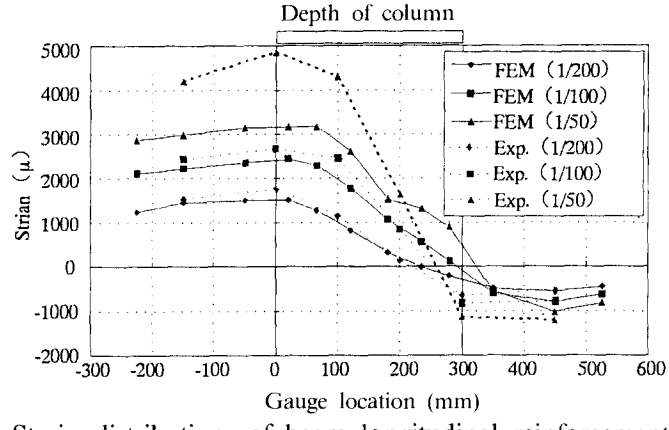

Fig. 9 Strain distributions of beam longitudinal reinforcement, OKJ3.

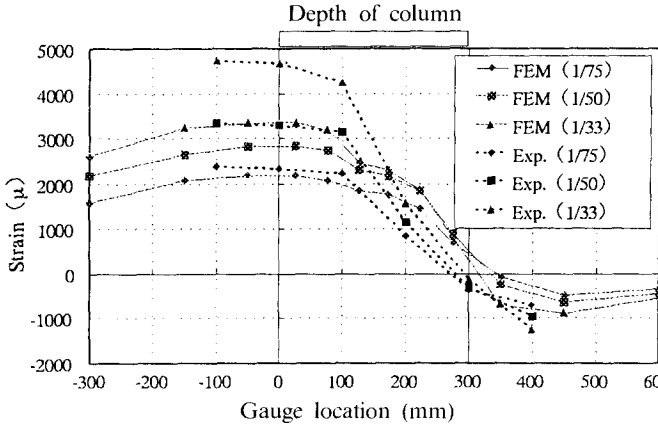

Fig. 10 Strain distributions of beam longitudinal reinforcement, I2.

the joint at each story drift of specimens OKJ3 and I2 are shown in Figs. 9 and 10. The analytical results gave a good agreement with the experimental result nearly at the story drift angle of $Rs=1/100$ rad.. But the analytical strains in tensile reinforcement in the latter term resulted in small compared with experiment. It is considered that the local flexural crack on the critical section of the beam and the slippage of beam longitudinal reinforcement through a joint were not represented using the smeared rack model.

Fig. 11 shows the analytical strain in the joint lateral reinforcement of specimen OKJ3. The analytical strain in the early term resulted in small compared with experiment. And the analytical results in the latter term gave a good agreement with the experimental result.

3.3. Internal stress flow

Fig. 12 shows the principal compressive stress contours of the joint concrete of specimen OKJ3. The arch mechanisms of beams and columns, and the diagonal compressive strut mechanism along the joint were observed on the stress contours of concrete. The strut concrete stresses

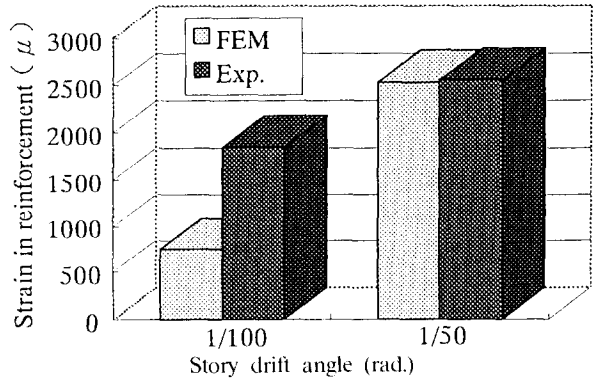

Fig. 11 Strain in lateral reinforcement in the joint, OKJ3.

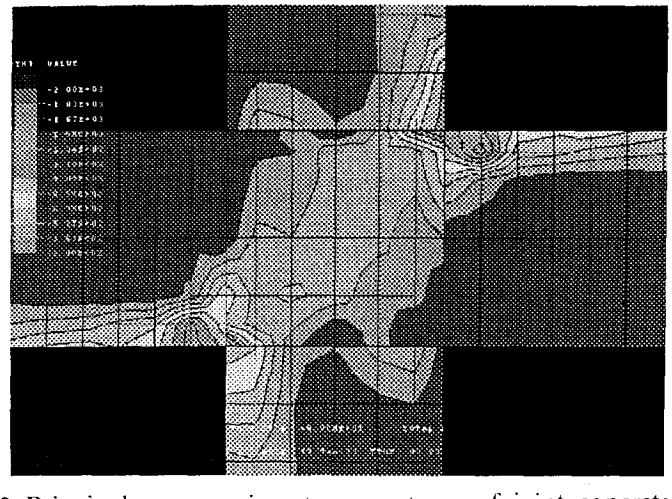

Fig. 12 Principal compressive stress contours of joint concrete, OKJ3.

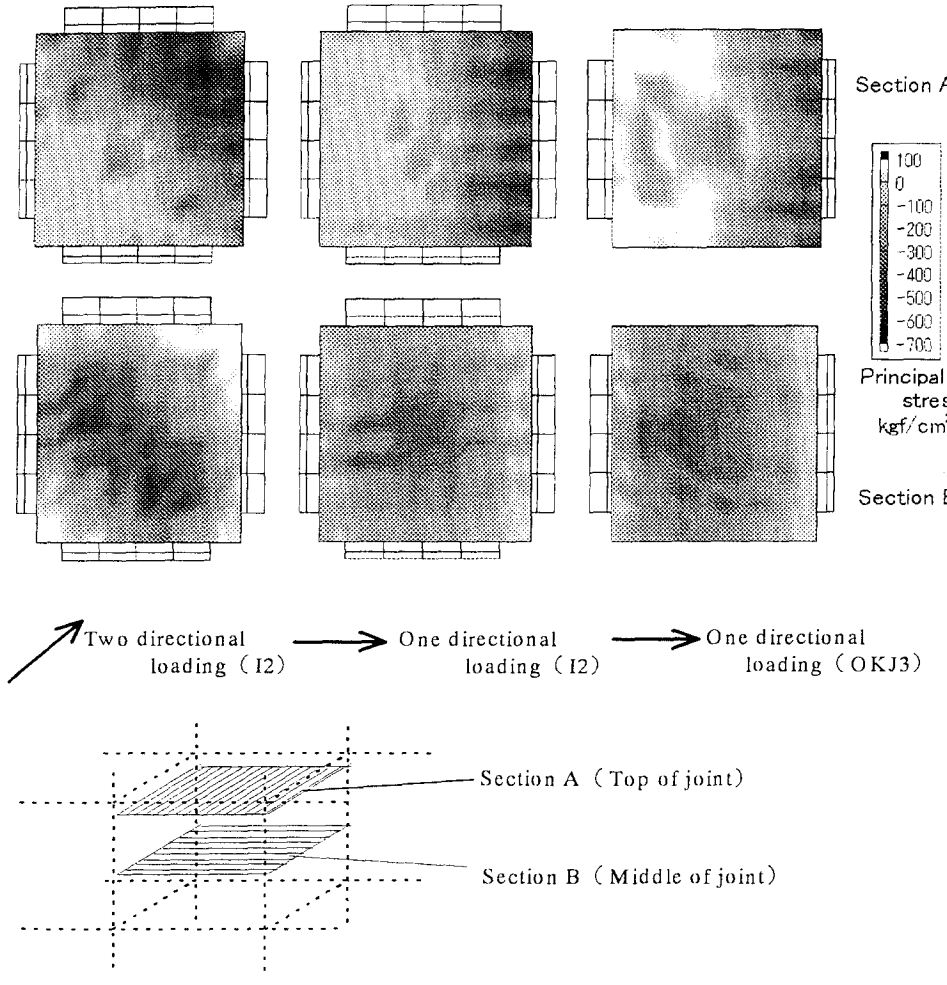

Fig. 13 Principal compressive stress contours of joint concrete, OKJ3 and I2.

of the joint were from 36 to 52 MPa at the maximum story shear force. These stresses were about 40 percent of the concrete compressive strength.

Fig. 13 shows the principal compressive stress contours on the horizontal section of the joint concrete of specimens OKJ3 and I2 nearly at the story drift angle of 1/100 rad.. Though the compressive stress is concentrated at the center on the middle section of the joint (section B), it is concentrated near at the beam critical section (at right side) on the top section of the joint (section A). From this observation, it is recognized that the inclined compressive struts are formed. As for specimen I2, in the case under two-directional loading, the compressive stresses are transferred uniformly and widely in the joint to two beams. But in the case under one-directional loading, the compressive strut width is decreased at the center of the joint from the wide compressive strut width at the area near to the beam. Also the effects of the transverse beams are not observed from the comparisons between specimens OKJ3 and I2 under one-directional loading.

4. Conclusions

The joint shear failure type plane interior joint OKJ3 and the beam flexural failure type 3-D joint I2 were analyzed using the nonlinear 3-D FEM program, and the hysteresis characteristics, failure mode, strain of reinforcements and internal stress flow were investigated. Though the analytical initial stiffness was higher than the test result, the analytical maximum strength and failure mode gave a reasonable agreement with the test results. From the analytical internal stress flow, the effects of the transverse beams and two-directional loading were recognized.

Acknowledgements

The work reported in this paper was sponsored by Grant-in Aid for Co-operative Research (No. 04302049, Representative Researcher: Professor H. Noguchi, Chiba University) and Encouragement of Young Scientists (No. 08750679, Representative Researcher: Research Associate T. Kashiwazaki, Chiba University) of the Ministry of Education, Science, Sports and Culture of Japanese Government.

The authors wish to express their gratitudes to members of co-operative research.

References

Architectural Institute of Japan (1990), *Design Guidelines for Earthquake Resistant Reinforced Concrete Buildings Based on Ultimate Strength Concept* (in Japanese).

Fafitis, A. and Shah, S. P. (1985), "Lateral reinforcement for high-strength concrete columns", *ACI SP-87*, 213-232.

Ihzuka, T. and Noguchi, H. (1992), "Nonlinear finite element analysis of reinforced concrete members with normal to high strength materials", *Proceedings of the Japan Concrete Institute*, **14**(6), 9-14 (in Japanese).

Kashiwazaki, T. and Noguchi, H. (1991), "Experimental study on the shear performance of R/C interior beam-column joints with ultra high-strength materials", *Proceedings of the Japan Concrete Institute*, **13**(2), 475-478 (in Japanese).

Kashiwazaki, T. and Noguchi, H. (1994), "Nonlinear finite element analysis on shear and bond of RC interior beam-column joints with ultra high-strength materials", *Transactions of the Japan Concrete Institute*, **16**, 509-516.

Kent, D. C. and Park, R. (1971), "Flexural members with confined concrete", *Journal of the Structural Division, Proceedings of the ASCE*, ST7, 1969-1990.

Lee, S., Kitayama, K., Otani, S. and Aoyama, H. (1992), "Shear strength of reinforced concrete interior beam-column joints using high-strength materials", *Proceedings of the Japan Concrete Institute*, **14**(2), 379-384 (in Japanese).

Uchida, K., Amemiya, A. and Noguchi, H. (1992), "Three-dimensional nonlinear finite element analysis for reinforced concrete members", *Summaries of Technical Papers of Annual Meeting of Architectural Institute of Japan*, Structures II, 1061-1064 (in Japanese).

Yonezawa, K. and Noguchi, H. (1994), "Analytical study on the shear performance of beam-column connections in hybrid structures", *Transactions of the Japan Concrete Institute*, **16**, 257-264.